

QCD corrections to lifetime differences of B_s mesons¹

Ulrich Nierste

Fermi National Accelerator Laboratory
Theory Division, MS106
IL 60510-500 Batavia, USA
E-mail: nierste@fnal.gov

Abstract

The calculation of QCD corrections to the width difference $\Delta\Gamma$ in the B_s -meson system is presented. The next-to-leading order corrections reduce the dependence on the renormalization scale significantly and allow for a meaningful use of hadronic matrix elements from lattice gauge theory. At present the uncertainty of the lattice calculations limits the prediction of $\Delta\Gamma$. The presented work has been performed in collaboration with Martin Beneke, Gerhard Buchalla, Christoph Greub and Alexander Lenz.

1 Introduction

Precision analyses of flavor-changing transitions are of experimental top priority in the forthcoming years. Decays of B mesons provide an especially fertile testing ground for various reasons: they allow for a high precision determination of three of the four parameters characterizing the Cabibbo-Kobayashi-Maskawa (CKM) matrix [1], including the CP-violating phase γ . Since flavor-changing transitions of B mesons are always suppressed by small CKM elements and heavy electroweak gauge boson masses, it is well possible that B physics experiments will reveal new physics. The large mass m_b of the b -quark further allows us to control hadronic uncertainties. Fermilab's CDF, D0 [2] and the planned BTeV [3] experiment prepare a dedicated B physics program. Other studies are in

¹Talk at *4th Workshop on Continuous Advances in QCD*, 12-14 May 2000, Minneapolis, Minnesota, USA

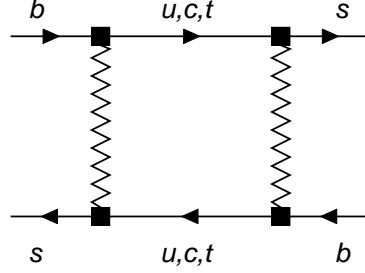


Figure 1: $B_s - \bar{B}_s$ mixing in the Standard Model. The zigzag lines represent W -bosons or charged pseudo-goldstone bosons.

progress at CLEO, LEP and at HERA-B [4] or planned for the future LHCb [5] experiment. While B -factories [6] only produce B_d, \bar{B}_d and B^\pm mesons, LEP and the hadron colliders also provide B_s mesons. Like their K , D and B_d counterparts B_s mesons mix with their antiparticles. Therefore the two mass eigenstates B_H and B_L (for “heavy” and “light”) are linear combinations of B_s and \bar{B}_s and differ in their mass and width. In the Standard Model $B_s - \bar{B}_s$ mixing is described in the lowest order by the box diagram depicted in Fig. 1. The dispersive part of the $B_s - \bar{B}_s$ mixing amplitude is called M_{12} . In the Standard Model it is dominated by box diagrams with internal top quarks. The absorptive part is denoted by Γ_{12} and mainly stems from box diagrams with light charm quarks. Γ_{12} is generated by decays into final states which are common to B_s and \bar{B}_s . While M_{12} can receive sizable corrections from new physics, Γ_{12} is induced by the CKM-favored tree-level decay $b \rightarrow c\bar{c}s$ and insensitive to new physics. Experimentally $B_s - \bar{B}_s$ mixing manifests itself in damped oscillations between the B_s and \bar{B}_s states which are governed by $M_{12} - i\Gamma_{12}/2$. We denote the mass and width differences between B_H and B_L by

$$\Delta m = M_H - M_L, \quad \Delta\Gamma = \Gamma_L - \Gamma_H.$$

By solving the eigenvalue problem of $M_{12} - i\Gamma_{12}/2$ one can relate Δm and $\Delta\Gamma$ to M_{12} and Γ_{12} :

$$\Delta m = 2|M_{12}|, \quad \Delta\Gamma = 2|\Gamma_{12}|\cos\phi, \quad (1)$$

where ϕ is defined as

$$\frac{M_{12}}{\Gamma_{12}} = - \left| \frac{M_{12}}{\Gamma_{12}} \right| e^{i\phi}. \quad (2)$$

Δm equals the $B_s - \bar{B}_s$ oscillation frequency and has not been measured yet, but we know the lower bound $\Delta m \geq 14.9 \text{ ps}^{-1}$ from LEP data [7]. It can be shown that this bound implies $|\Gamma_{12}|/|M_{12}| \ll$

0.01. In deriving (1) terms of order $|\Gamma_{12}/M_{12}|^2$ have been neglected. ϕ in (2) is a CP-violating phase, which is tiny in the Standard Model, so that $\Delta\Gamma_{SM} = 2|\Gamma_{12}|$. In the presence of new physics $\arg M_{12}$ and thereby ϕ can assume any value. ϕ can be measured from CP-asymmetries, which requires the resolution of the rapid $B_s - \bar{B}_s$ oscillations and tagging, i.e. the discrimination between B_s and \bar{B}_s mesons at the time $t = 0$ of their production. From (1) one verifies that a non-vanishing ϕ also affects $\Delta\Gamma$, which can be measured from untagged data samples and therefore involves better efficiencies than tagged studies. Unlike in the case of B_d mesons, the Standard Model predicts a sizable width difference $\Delta\Gamma$ in the B_s system, roughly between 5 and 30% of the average total width $\Gamma = (\Gamma_L + \Gamma_H)/2$. Now the decay of an untagged B_s meson into the final state f is in general governed by two exponentials:

$$\Gamma[f, t] \propto e^{-\Gamma_L t} |\langle f | B_L \rangle|^2 + e^{-\Gamma_H t} |\langle f | B_H \rangle|^2. \quad (3)$$

If f is a flavor-specific final state like $D_s^- \pi^+$ or $X \ell^+ \nu$, the coefficients of the two exponentials in (3) are equal. A fit of the corresponding decay distribution to a single exponential then determines the average width Γ up to corrections of order $(\Delta\Gamma)^2/\Gamma$. In the Standard Model CP violation in $B_s - \bar{B}_s$ mixing is negligible, so that we can simultaneously choose B_L and B_H to be CP eigenstates and the $b \rightarrow c\bar{c}s$ decay to conserve CP. Then B_H is CP-odd and cannot decay into a CP-even double-charm final state f_{CP+} like $(J/\psi\phi)_{L=0,2}$, where L denotes the quantum number of the orbital angular momentum. Thus a measurement of the B_s width in $B_s \rightarrow f_{CP+}$ determines Γ_L . By comparing the two measurements one finds $\Delta\Gamma/2$. In the presence of a non-zero CP-violating phase ϕ this procedure measures [8]

$$\Delta\Gamma \cos \phi = \Delta\Gamma_{SM} \cos^2 \phi. \quad (4)$$

The extra factor of $\cos \phi$ stems from the fact that in the presence of CP violation both B_L and B_H can decay into f_{CP+} . CDF will perform this measurement with $B_s \rightarrow D_s^- \pi^+$ and $B_s \rightarrow J/\psi\phi$ in Run-II of the Tevatron [9].

2 QCD effects

The $B_s - \bar{B}_s$ mixing amplitude of Fig. 1 and the B_s decay amplitude are affected by strong interaction effects. $\Delta\Gamma_{SM} = 2|\Gamma_{12}|$ involves various different mass scales and the the QCD corrections associated with these scales require different treatments. In the first step an operator product expansion at the scale M_W is performed to integrate out the W -boson. The Standard Model $b \rightarrow c\bar{c}s$ amplitude is matched to its counterpart in an effective field theory in which $\Delta B = 1$ transitions (B is the bottom number) are described by four-quark operators. The corresponding effective hamiltonian reads

$$\mathcal{H}_{eff} = \frac{G_F}{\sqrt{2}} V_{cb}^* V_{cs} \left(\sum_{r=1}^6 C_r Q_r + C_8 Q_8 \right), \quad (5)$$

with the operators

$$Q_1 = (\bar{b}_i c_j)_{V-A} (\bar{c}_j s_i)_{V-A} \quad Q_2 = (\bar{b}_i c_i)_{V-A} (\bar{c}_j s_j)_{V-A}, \quad (6)$$

$$Q_3 = (\bar{b}_i s_i)_{V-A} (\bar{q}_j q_j)_{V-A} \quad Q_4 = (\bar{b}_i s_j)_{V-A} (\bar{q}_j q_i)_{V-A}, \quad (7)$$

$$Q_5 = (\bar{b}_i s_i)_{V-A} (\bar{q}_j q_j)_{V+A} \quad Q_6 = (\bar{b}_i s_j)_{V-A} (\bar{q}_j q_i)_{V+A}, \quad (8)$$

$$Q_8 = \frac{g}{8\pi^2} m_b \bar{b}_i \sigma^{\mu\nu} (1 - \gamma_5) T_{ij}^a s_j G_{\mu\nu}^a. \quad (9)$$

Here the i, j are colour indices and a summation over $q = u, d, s, c, b$ is implied. $V \pm A$ refers to $\gamma^\mu(1 \pm \gamma_5)$ and $S - P$ (which we need below) to $(1 - \gamma_5)$. The current-current operators Q_1 and Q_2 stem from W -boson exchange between the $\bar{b}c$ and $\bar{c}s$ lines. Q_{3-6} are four-quark penguin operators and Q_8 is the chromomagnetic penguin operator. The Wilson coefficients C_i contain the short-distance physics and are functions of the heavy W and top quark masses. Since they do not depend on long-distance QCD effect, they can be calculated in perturbation theory. C_{3-6} are very small. The matching calculation determines the C_i 's at a high renormalization scale $\mu = \mathcal{O}(M_W)$. The renormalization group (RG) evolution of the coefficients down to $\mu = \mathcal{O}(m_b)$ sums the large logarithm $\alpha_s \ln(M_W/m_b)$ to all orders in perturbation theory. The operator product expansion leading to (5) and the RG improvement amount to a simultaneous expansion in m_b^2/M_W^2 , $\alpha_s(M_W)$ and $\alpha_s(m_b)$ of the $b \rightarrow c\bar{c}s$ amplitude. \mathcal{H}_{eff} in (5) reproduces the leading term in the power expansion in m_b^2/M_W^2 .

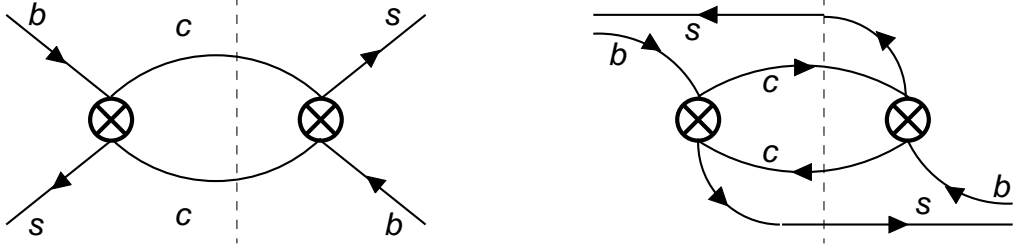
The second step to predict $\Delta\Gamma_{SM}$ involves an operator product expansion at the scale m_b . The corresponding formalism has been formulated long ago by the hosts of this conference [10]. The starting point for the calculation of the widths Γ_H of some b -flavored hadron H is the optical theorem, which relates Γ_H to the absorptive part of the forward scattering amplitude of H . Neglecting CP violation in the decay amplitude the optical theorem implies

$$\Gamma_H \propto \text{Im} \langle H | i \int d^4x T \mathcal{H}_{eff}(x) \mathcal{H}_{eff}(0) | H \rangle. \quad (10)$$

Now the *Heavy Quark Expansion* (HQE) [10] is an operator product expansion of the forward scattering amplitude in (10). Schematically

$$\Gamma_H \propto G_F^2 \sum_j m_b^{8-d_j} F_j(\mu/m_b) \underbrace{\langle H | \mathcal{O}_j(\mu) | H \rangle}_{\mathcal{O}(\Lambda_{QCD}^{d_j-3})} \quad (11)$$

Here new Wilson coefficients F_j have appeared. They contain the physics associated with scales above the matching scale $\mu = \mathcal{O}(m_b)$, at which the HQE is performed. The \mathcal{O}_j 's are local operators

Figure 2: Leading-order diagrams for Γ_{12}

with dimension $d_j \geq 3$. The HQE is a simultaneous expansion of Γ_H in Λ_{QCD}/m_b and $\alpha_s(m_b)$. Increasing powers of Λ_{QCD}/m_b correspond to increasing dimensions d_j of the local operators \mathcal{O}_j .

To calculate $\Delta\Gamma$ from the HQE one must extend the above formalism to the two state system (B_s, \bar{B}_s) :

$$\Delta\Gamma_{SM} = 2|\Gamma_{12}| = -\frac{1}{M_{B_s}} \text{Im} \langle \bar{B}_s | i \int d^4x T \mathcal{H}_{eff}(x) \mathcal{H}_{eff}(0) | B_s \rangle \quad (12)$$

The corresponding leading-order diagrams are shown in Fig. 2. (12) is matched to local operators in analogy to (11):

$$\begin{aligned} & \text{Im} \langle \bar{B}_s | i \int d^4x T \mathcal{H}_{eff}(x) \mathcal{H}_{eff}(0) | B_s \rangle \\ &= -\frac{G_F^2 m_b^2}{12\pi} |V_{cb}^* V_{cs}|^2 \cdot \\ & \left[F \left(\frac{m_c^2}{m_b^2} \right) \langle \bar{B}_s | Q | B_s \rangle + F_S \left(\frac{m_c^2}{m_b^2} \right) \langle \bar{B}_s | Q_S | B_s \rangle \right] \left[1 + \mathcal{O} \left(\frac{\Lambda_{QCD}}{m_b} \right) \right]. \end{aligned} \quad (13)$$

The HQE for the $\Delta B = 2$ transition in (12) requires four-quark operators involving both the b -quark and the s -quark field, i.e. operators with dimension six or higher. The two dimension-6 operators appearing in (13) are

$$Q = (\bar{b}_i s_i)_{V-A} (\bar{b}_j s_j)_{V-A}, \quad Q_S = (\bar{b}_i s_i)_{S-P} (\bar{b}_j s_j)_{S-P}. \quad (14)$$

In the leading order of QCD the RHS of (13) is pictorially obtained by simply shrinking the (c, \bar{c}) loop in Fig. 2 to a point. The Wilson coefficients F and F_S also depend on the charm quark mass m_c , which is formally treated as a hard scale of order m_b , since $m_c \gg \Lambda_{QCD}$. Strictly speaking, the HQE in (13) is an expansion in $\Lambda_{QCD}/\sqrt{m_b^2 - 4m_c^2}$. For the calculation of F and F_S it is crucial that these

coefficients do not depend on the infrared structure of the process. In particular they are independent of the QCD binding forces in the external B_s and \bar{B}_s states in (13), so that they can be calculated in perturbation theory at the parton level. The non-perturbative long-distance QCD effects completely reside in the hadronic matrix elements of Q and Q_S .

The third and final step in the prediction of $\Delta\Gamma_{SM}$ is the calculation of the hadronic matrix elements with non-perturbative methods such as lattice gauge theory. It is customary to parametrize these matrix elements as

$$\begin{aligned}\langle \bar{B}_s | Q | B_s \rangle &= \frac{8}{3} f_{B_s}^2 M_{B_s}^2 B \\ \langle \bar{B}_s | Q_S | B_s \rangle &= -\frac{5}{3} f_{B_s}^2 M_{B_s}^2 \frac{M_{B_s}^2}{(\bar{m}_b + \bar{m}_s)^2} B_S.\end{aligned}\tag{15}$$

In the so called vacuum insertion approximation B and B_S are equal to 1.

3 Next-to-leading order QCD corrections to $\Delta\Gamma$

The discussion of $\Delta\Gamma$ in sect. 2 has been restricted to the leading order (LO) of QCD [11]. The only QCD effects included in this order are the leading logarithms $\alpha_s^n \ln^n(M_W/m_b)$, $n = 0, 1, 2, \dots$, contained in the C_j 's of the effective $\Delta B = 1$ hamiltonian in (5). To predict $\Delta\Gamma$ with next-to-leading order (NLO) accuracy one must first include the corrections of order $\alpha_s^{n+1} \ln^n(M_W/m_b)$, $n = 0, 1, 2, \dots$, to these coefficients [12]. Second corrections of order $\alpha_s(m_b)$ must be included in F and F_S [13]. This step requires the inclusion of hard gluon exchange on both sides of (13). The corresponding diagrams are depicted in Fig. 3. The motivations for this cumbersome calculation are

1. to verify the infrared safety of F and F_S ,
2. to allow for an experimental test of the HQE,
3. a meaningful use of lattice results for hadronic matrix elements,
4. to reduce the sizable μ -dependence of the LO,
5. a consistent use of $\Lambda_{\overline{MS}}$,
6. the large size of QCD corrections, typically of order 30%.

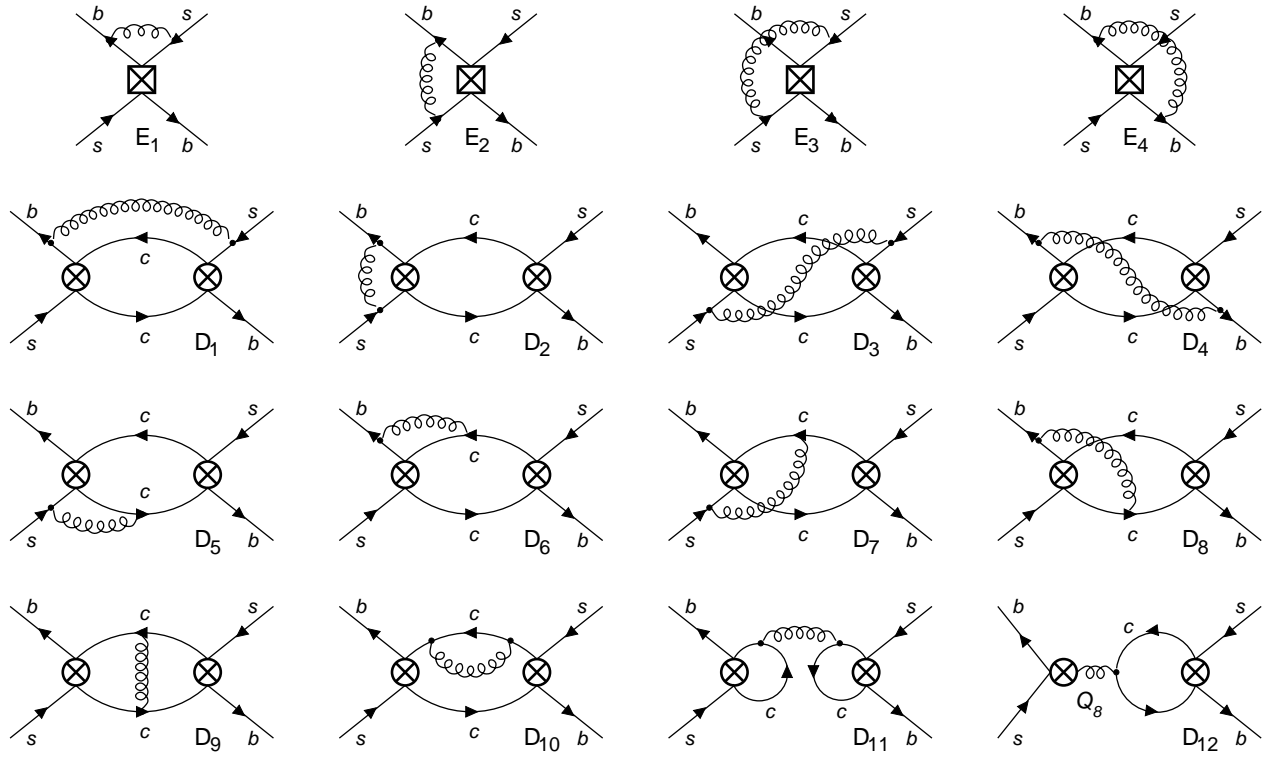


Figure 3: QCD corrections to $\Delta\Gamma$. NLO corrections to diagrams with the penguin operators Q_{3-6} are negligible.

We will now comment on these points: A necessary condition for the validity of any operator product expansion is the disappearance of all infrared regulators from the Wilson coefficients. From our explicit calculation we have verified that this is indeed the case at order α_s . We found IR-singularities to cancel via two mechanisms:

- Bloch-Nordsieck cancellations among different cuts of the same diagram,
- factorization of IR-singularities, which end up in $\langle \bar{B}_s | \mathcal{O} | B_s \rangle$, $\langle \bar{B}_s | \mathcal{O}_S | B_s \rangle$.

Early critics of the HQE had found power-like infrared divergences in individual cuts of diagrams. In response the cancellation of these divergences has been shown [14], long ago before we have performed the full NLO calculation. The second type of IR-cancellations occurs between the diagrams in the first and second row of Fig. 3. Thus when the external meson states in (13) are replaced by quark states, both sides of the equation are infrared divergent. Yet the IR-divergences factorize rendering F and F_S infrared safe. Point 2 above addresses the conceptual basis of the HQE, which

is sometimes termed *quark-hadron duality*. It is not clear, whether the HQE reproduces all QCD effects completely. Exponential terms like $\exp(-\kappa m_b/\Lambda_{QCD})$, for example, cannot be reproduced by a power series. [15] The relevance of such corrections to the HQE can at present only be addressed experimentally, by confronting HQE-based predictions with data. The only QCD informations contained in the LO prediction for $\Delta\Gamma$ are the coefficients of $\alpha_s^n \ln^n M_W$, associated with hard gluon exchange along the W -mediated $b \rightarrow c\bar{c}s$ amplitude. The question of quark-hadron duality, however, has nothing to do with these logarithmic terms. A meaningful test of this aspect of the HQE therefore requires a NLO calculation, which includes non-logarithmic terms of order α_s . In view of the success of the HQE in accurately measured B physics observables it is conceivable that the uncertainty due to violations of quark-hadron duality is well below the uncertainty from the non-perturbative calculation of the hadronic B -parameters. At present lattice calculation of B and B_s [16] are only possible in the quenched approximation, neglecting the effect of dynamical fermions. Unquenched calculations of f_{B_s} are now available, but still a new subject in the field [17]. The third point in our list above refers to the fact that QCD predictions obtained on the lattice must be matched to the continuum. This involves the calculation of the diagrams in the first row on Fig. 3 in lattice perturbation theory. A meaningful prediction for $\Delta\Gamma$ with a proper cancellation of the renormalization scale and scheme dependences between F, F_S and B, B_S then requires a full NLO calculation. The renormalization scale μ is an unphysical parameter and observables do not depend on μ . The truncation of the perturbation series, however, introduces a μ -dependence, which diminishes order-by-order in α_s . As mentioned in point 4, the LO result for $\Delta\Gamma$ suffers from a huge scale dependence, which is substantially reduced in the NLO prediction. Further a LO calculation cannot use the fundamental QCD scale parameter $\Lambda_{\overline{MS}}$ [18], which is an intrinsic NLO quantity. Finally, as mentioned in point 6, the calculated QCD corrections are sizable, of the order of 30%, and therefore necessary to keep up with the precision of the forthcoming experiments.

Including corrections of order Λ_{QCD}/m_b [19] to (13) we predict [13]

$$\left(\frac{\Delta\Gamma_{SM}}{\Gamma}\right)_{B_s} = \left(\frac{f_{B_s}}{245 \text{ MeV}}\right)^2 [0.008 B + 0.204 B_S - 0.086]$$

with B and B_S defined in the \overline{MS} -scheme at $\mu = m_b$. With [16]

$$B(\mu = m_b) = 0.80 \pm 0.15, \quad B_S(\mu = m_b) = 1.19 \pm 0.20$$

one finds

$$\left(\frac{\Delta\Gamma}{\Gamma}\right)_{B_s} = \left(\frac{f_{B_s}}{245 \text{ MeV}}\right)^2 (0.162 \pm 0.041 \pm ???). \quad (16)$$

The questions marks address the unknown error from the quenching approximation.

If $\Delta\Gamma$ is found below the Standard Model prediction, it will be interesting to find out, whether this is due to a breakdown of the HQE prediction in (16) or a new CP-violating phase ϕ in (4). To this end we note that one can determine ϕ without using the theory prediction for $\Delta\Gamma_{SM}$, even from untagged data alone [8, 20]. Further the HQE prediction for other width differences, e.g. between the B^+ and B_d or between the B_s and B_d mesons, involve a similar structure than the prediction for $\Delta\Gamma$. The corresponding diagrams are similar to those in Fig. 2 and Fig. 3, but involve $\Delta B = 0$ transitions [10, 19]. The width difference between B^+ and B_d is insensitive to new physics and therefore directly tests the HQE and the lattice calculations of hadronic matrix elements. The small width difference between B_s and B_d is mildly sensitive to new physics from penguin contributions [21].

Acknowledgments

I thank Misha Voloshin for inviting me to this beautiful workshop and for the hospitality at his institute. I am grateful for many stimulating discussions with the participants.

References

- [1] N. Cabibbo, Phys. Rev. Lett. **10** (1963) 531. M. Kobayashi and T. Maskawa, Prog. Theor. Phys. **49** (1973) 652.
- [2] K. Pitts (for Fermilab D0 and CDF collab.), Proceedings of the 4th Workshop on Heavy Quarks at Fixed Target (HQ 98), Batavia, USA, 1998.
- [3] R. W. Gardner (BTeV Collaboration), Nucl. Instrum. Meth. **A446** (2000) 208.
- [4] P. Krizan et al., *HERA-B, an experiment to study CP violation at the HERA proton ring using an internal target*, Nucl. Instrum. Meth. **A351** (1994) 111.
- [5] David Websdale, *LHCb: A dedicated B physics detector for the LHC*, Nucl. Phys. Proc. Suppl. **50** (1996) 333.
- [6] D. Boutigny et al., *BaBar technical design report*, SLAC-R-0457. M.T. Cheng et al. (Belle collab.), *A study of CP violation in B meson decays: Technical design report*, BELLE-TDR-3-95.
- [7] A. Stocchi, talk at *ICHEP 2000 conference*, 7 Jul - 2 Aug 2000, Osaka, Japan.
- [8] Y. Grossman, Phys. Lett. **B380** (1996) 99.

- [9] F. Azfar, L. Lyons, M. Martin, C. Paus and J. Tseng, CDF note no. 5351.
- [10] M. Voloshin and M. Shifman, Sov. J. Nucl. Phys. **41** (1985) 120; J. Chay, H. Georgi and B. Grinstein, Phys. Lett. **B247** (1990) 399. I.I. Bigi, N.G. Uraltsev and A.I. Vainshtein, Phys. Lett. **B293** (1992) 430 [(E) Phys. Lett. **B297** (1993) 477]; I.I. Bigi, M. Shifman, N.G. Uraltsev, and A. Vainshtein, Phys. Rev. Lett. **71** (1993) 496. A.V. Manohar and M.B. Wise, Phys. Rev. **D49** (1994) 1310; B. Blok, L. Koyrakh, M. Shifman and A.I. Vainshtein, Phys. Rev. **D49** (1994) 3356; T. Mannel, Nucl. Phys. **B413** (1994) 396. M. Neubert and C. T. Sachrajda, Nucl. Phys. **B483** (1997) 339.
- [11] J.S. Hagelin, Nucl. Phys. **B193**, 123 (1981); E. Franco, M. Lusignoli and A. Pugliese, Nucl. Phys. **B194**, 403 (1982); L.L. Chau, Phys. Rep. **95**, 1 (1983); A.J. Buras, W. Słominski and H. Steger, Nucl. Phys. **B245**, 369 (1984); M.B. Voloshin, N.G. Uraltsev, V.A. Khoze and M.A. Shifman, Sov. J. Nucl. Phys. **46**, 112 (1987); A. Datta, E.A. Paschos and U. Türke, Phys. Lett. **B196**, 382 (1987); A. Datta, E.A. Paschos and Y.L. Wu, Nucl. Phys. **B311**, 35 (1988).
- [12] A. J. Buras and P. H. Weisz, Nucl. Phys. **B333** (1990) 66. A.J. Buras, M. Jamin, M.E. Lautenbacher and P.H. Weisz, Nucl. Phys. **B370**, 69 (1992); Addendum-ibid. **B375**, 501 (1992).
- [13] M. Beneke, G. Buchalla, C. Greub, A. Lenz and U. Nierste, Phys. Lett. **B459** (1999) 631.
- [14] I. Bigi and N. Uraltsev, Phys. Lett. **B280**, 271 (1992).
- [15] *see e.g.* M. Shifman, hep-ph/9505289.
- [16] S. Hashimoto, K. I. Ishikawa, T. Onogi and N. Yamada, Phys. Rev. **D62** (2000) 034504.
- [17] S. Hashimoto, Nucl. Phys. Proc. Suppl. **83-84** (2000) 3.
- [18] W. A. Bardeen, A. J. Buras, D. W. Duke and T. Muta, Phys. Rev. **D18** (1978) 3998.
- [19] M. Beneke, G. Buchalla and I. Dunietz, Phys. Rev. **D54** (1996) 4419.
- [20] I. Dunietz, R. Fleischer and U. Nierste, *in preparation*.
- [21] Y. Keum and U. Nierste, Phys. Rev. **D57** (1998) 4282.